ChemPubSoc Europe

DOI: 10.1002/chem.201406493

CHEMISTRY A European Journal Full Paper

Peptidomimetics

Design and Stereoselective Synthesis of ProM-2: A Spirocyclic Diproline Mimetic with Polyproline Type II (PPII) Helix Conformation

Cédric Reuter,[a] Robert Opitz,[b] Arne Soicke,[a] Stephan Dohmen,[a] Matthias Barone,[b] Slim Chiha,[a] Marco Tobias Klein,[a] Jörg-Martin Neudörfl,[a] Ronald Kühne,*[b] and Hans-Günther Schmalz*[a]

Abstract: With the aim of developing polyproline type II helix (PPII) secondary-structure mimetics for the modulation of prolin-rich-mediated protein–protein interactions, the novel diproline mimetic ProM-2 was designed by bridging the two pyrrolidine rings of a diproline (Pro–Pro) unit through a *Z*-vinylidene moiety. This scaffold, which closely resembles a section of a PPII helix, was then stereoselectively synthesized by exploiting a ruthenium-catalyzed ring-closing metathesis (RCM) as a late key step. The required vinylproline building blocks, that is, (*R*)-*N*-Boc-2-vinylproline (Boc = *tert*-butyloxycarbonyl) and (*S,S*)-5-vinylproline-*tert*-butyl ester, were prepared on a gram scale as pure stereoisomers. The difficult peptide coupling of the sterically demanding building blocks was achieved in good yield and without epimerization by using 2-(1*H*-7-azabenzotriazol-1-yl)-1,1,3,3-tetramethyluronium hexafluorophosphate (HATU)/*N*,*N*-diisopropylethylamine (DIPEA). The RCM proceeded smoothly in the presence of the Grubbs II catalyst. Stereostructural assignments for several intermediates were secured by X-ray crystallography. As a proof of concept, it was shown that certain peptides containing ProM-2 exhibited improved (canonical) binding towards the Ena/VASP homology 1 (EVH1) domain as a relevant protein interaction target.

Introduction

The search for small molecules that allow the selective modulation of pharmacologically relevant protein–protein interactions has become an important challenge in chemical biology and medicinal chemistry.[1] Once the active conformation of short peptide sequences, which usually take over this function in nature, has been determined, it is, in principle, possible to design and synthesize geometrically defined peptide mimetics[2] to target such interactions.[3] As an important example, proline-rich recognizing domains (PRDs) are able to selectively bind to proline-rich motifs (PRMs) in a structurally well-understood fashion.[4] These protein–protein interactions play an important role in a variety of relevant cellular processes, such as tyrosine kinase receptor signaling,[5] endocytosis,[6] cytoskeletal rearrangements,[7] transcription,[8] and splicing,[9] and represent challenging targets for the development of small molecules that act as specific inhibitors/modulators of such interactions by mimicking the PRM in the active conformation.

A constitutive property of all PRMs is that their core motif needs to adopt a left-handed polyproline type II (PPII) helix conformation to be recognized by the respective PRD. PPII helices are characterized by a complete lack of main-chain hydrogen bonding and exhibit a helical pitch of 9.3 Å (three residues per turn) with Φ and Ψ angles of about -75 and 145°, respectively.[10] Based on this information, we recently introduced the "rationally designed" scaffold ProM-1 as a rigid diproline analogue that displayed a virtually perfect PPII conformation (Figure 1).[11,12] Herein, we now report the design and synthesis of a second PPII-structured dipeptide mimetic, that is, the spirocyclic scaffold ProM-2, as an alternative module (Pro–Pro substitute) for the development of geometrically defined PRD-binding small molecules.

[a] *Dr. C. Reuter, Dr. A. Soicke, S. Dohmen, S. Chiha, M. T. Klein, Dr. J.-M. Neudörfl, Prof. Dr. H.-G. Schmalz*
Department of Chemistry, University of Cologne
Greinstrasse 4, 50939 Cologne (Germany)
E-mail: schmalz@uni-koeln.de

[b] *Dr. R. Opitz, M. Barone, Dr. R. Kühne*
Leibniz-Institut für Molekulare Pharmakologie (FMP)
Campus Berlin-Buch, Robert-Rössle-Str. 10
13125 Berlin (Germany)
E-mail: kuehne@fmp-berlin.de

Supporting information for this article is available on the WWW under http://dx.doi.org/10.1002/chem.201406493.

Results and Discussion

Design

Taking a model of a Pro–Pro unit in a PPII helix conformation as a starting point, we recognized that the geometry could be locked by stereoselectively introducing a stiff vinylidene bridge between the two pyrrolidine rings. Initially, this led to the design of the scaffold ProM-1 (Figure 1),[12] which was subse-

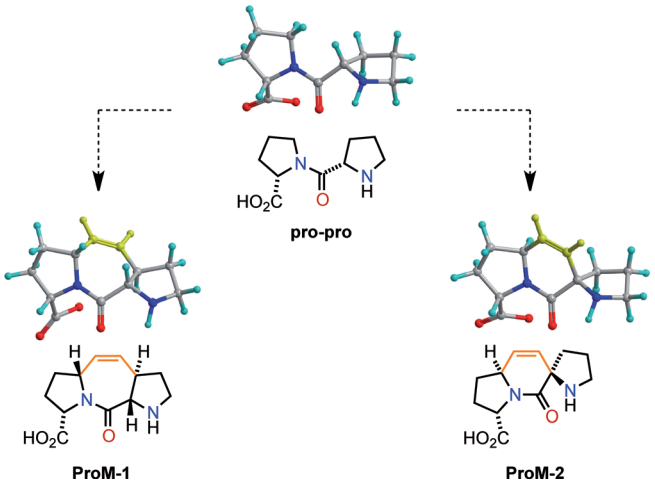

Figure 1. Design of the PPII Pro–Pro mimetics ProM-1 (previous work)[11,12] and ProM-2 (this work). In both structures, the diproline unit is locked in a virtually perfect PPII helix conformation.

quently incorporated as a Pro–Pro substitute into the core motif of a PRM ligand binding to the SH3 domain.[12a] Indeed, the resulting ProM-1-containing peptides exhibited pronounced binding affinity to the PRD target (SH3 domain). Thus, we could demonstrate (for the first time) that it was possible to modify the core motif of a proline-rich ligand without complete loss of affinity.[12a]

More recently, we turned our attention to the Ena/VASP (vasodilator-stimulated phosphoprotein) proteins as a relevant target for the design of PRD-binding ligands. Ena/VASP protein family members are multifunctional regulators involved in the remodeling of the actin cytoskeleton,[13] that is, fundamental cellular processes, including axon guidance and cell migration. All Ena/VASP proteins contain an Ena/VASP homology 1 (EVH1) domain specialized in recognizing PRMs as natural interaction partners.[4a,5c] A pathological ligand is the protein ActA of the intracellular pathogen *Listeria monocytogenes*, which is known for causing listeriosis in mammals.[14] In this particular case, the Ena/VASP-EVH1 domain recognizes four sequence sections of ActA that all contain a **FPxxP** motif and satisfy the consensus motif (F/W)PxϕP of the Ena/VASP-EVH1 domains, in which x represents any amino acid and ϕ is any aliphatic amino acid.[5a,c] Notably, the first and last proline residues are essential for binding, and therefore, are highly conserved in the partner proteins of Ena/VASP-EVH1 domains. Starting with the ActA-derived peptide Ac-^{332}SFEFPPPPTEDEL-NH_2, we tried to replace pairs of prolines in the ActA-derived model ligand by ProM-1. We found that Ac-SFE-**FPP[ProM-1]**-TEDEL-NH_2 showed improved binding to the EVH1 domain of VASP and all four prolines could even be substituted for ProM-1 (i.e., Ac-SFE-**F[ProM-1][ProM-1]**-TEDEL-NH_2) without loss of affinity relative to the wild-type peptide. However, substitution of the first two prolines by ProM-1 (i.e., Ac-SFE-**F[ProM-1]PP**-TEDEL-NH_2) resulted in a decrease of the binding affinity to the VASP-EVH1 domain.[15]

To understand these observations, we investigated the interaction of the ProM-1-containing peptides with the EVH1 domain by means of molecular modeling.[16] As depicted in Figure 2, the model suggested that the decreased binding affinity of the peptide with the **F[ProM-1]PP** core resulted from an unfavorable steric interaction between the vinylidene bridge of ProM-1 and the protein surface, leading to a partial displacement of the ligand (see Figure 2a and b). To avoid this unfavorable interaction, a different Pro–Pro mimetic (still rigidified in a PPII conformation, but with a different backbone geometry) was required. After re-analyzing the model of the parent PPII diproline structure, we found that rigidification could also be achieved by introducing a vinylidene bridge between the two pyrrolidine rings in a different manner. Thus, the spirocyclic scaffold ProM-2 was conceived (Figure 1). The computational model suggested that the introduction of ProM-2 as a substitute for the first two proline units of the core motif of the ActA-derived ligand (i.e., **F-[ProM-2]-PP**) should lead to a better fit (i.e., a closer contact) to the binding site, and therefore, to a higher binding affinity (Figure 2c and d).

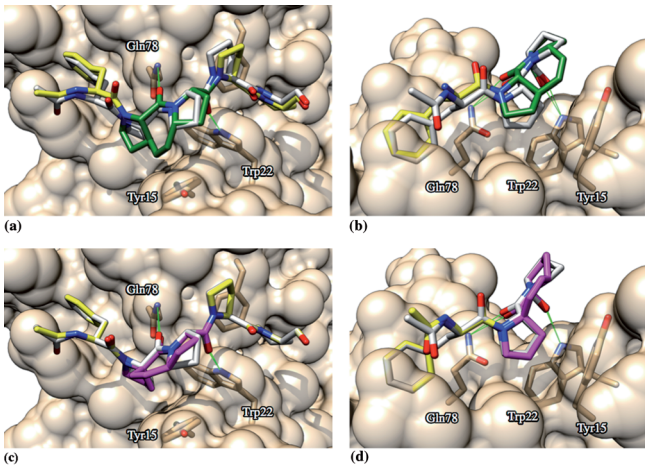

Figure 2. Calculated superimposed molecular models (in two perspectives) of the core regions of PRM ligands binding to the Ena/VASP-EVH1 domain. Wild-type ligand **FPPPP** (a; gray) and the synthetic ligand **F[ProM-1]PP** (b; yellow with ProM-1 shown in green); wild-type ligand **FPPPP** (c; gray) and the synthetic ligand **F[ProM-2]PP** (d; yellow with ProM-2 shown in magenta). The models are based on the crystal structure 1evh[17] of the EnaH-EVH1 domain and on crystal structures of ProM-1 and ProM-2.

Synthesis

To synthesize the ProM-2 scaffold (as its fluorenylmethyloxycarbonyl (Fmoc)-protected derivative **1**), we decided to follow a metathesis-based strategy related to that previously used for the synthesis of other ProMs.[12] As shown in Scheme 1, retrosynthetic analysis leads to a dipeptidic precursor of type **2**, which, in turn, is derived from two vinylproline building blocks of types **3** and **4** (Scheme 1).

The synthesis of a *trans*-5-propenylproline building block of type **3** (Scheme 2) started from L-proline (**5**, >99% *ee*), which was first double-protected by treatment with an excess of methyl chloroformate in the presence of NEt_3 to give the carbamate/ester **6** in 88% yield.[12b] Functionalization at C-5 was

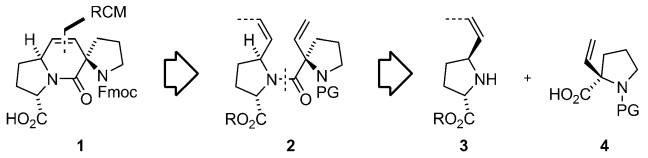

Scheme 1. Strategy (retrosynthetic analysis) for the synthesis of **1** based on ring-closing metathesis (RCM); PG = protecting group.

then initiated by electrochemical oxidation of **6** using graphite plate electrodes (48×28 mm, 600 mA, 5 mm, 0 °C) in a 0.05 M solution of Bu_4NBF_4 in methanol.[12b,18] Without any purification, the resulting N,O-acetal **7**, which was obtained in nearly quantitative yield as a 1:1 mixture (GC-MS) of diastereomers, was further converted into the 5-propenylproline derivative **8** in 66% yield through a BF_3-mediated reaction with a cuprate prepared in situ from the corresponding Grignard reagent.[19] One can assume that the reaction proceeds through diastereoselective attack of the cuprate at an intermediate N-acyliminium ion. Notably, product **8** was obtained with virtually perfect *trans* selectivity (as a 9:1 mixture of the *Z/E* isomers) by using the Grignard reagent freshly prepared from (*Z*)-1-bromopropene.[20]

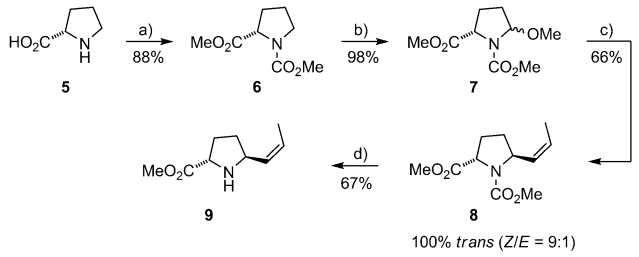

Scheme 2. Synthesis of **9**. a) $ClCO_2Me$ (3.5 equiv), NEt_3 (3.0 equiv), MeOH, RT, 15 h; b) $-2e^-$ (600 mA, 5 mm), Bu_4NBF_4, MeOH, 0 °C; c) $BrMgCH{=}CHCH_3$, $CuBr{\cdot}SMe_2$, Et_2O, −40 °C, then addition of $BF_3{\cdot}Et_2O$ and **7** at −78 °C to 10 °C; d) TMSI (2 equiv), CH_2Cl_2, reflux, 3 h.

Finally, selective monodeprotection of **8** (cleavage of the methyl carbamate functionality) was achieved with iodotrimethylsilane (TMSI) in dichloromethane[21] to afford the *trans*-5-propenylproline ester **9** (*Z/E* = 9:1) in 38% yield over four steps on a gram scale. The relative (and absolute) configuration of (*Z*)-**9** was unequivocally proven by means of X-ray crystal-structure analysis of its hydro iodide salt (see the Supporting Information).

Preparation of the second building block, that is, the 2-vinylproline derivative **12**, was achieved as shown in Scheme 3 by slightly modifying the synthesis of Bittermann and Gmeiner.[22]

First, L-proline (**5**) was protected by treatment with chloral[23] and the resulting cyclic N,O-acetal was formylated (lithium diisopropylamide (LDA), HCO_2Me) to diastereoselectively[24] give the aldehyde **10** in 54% yield over two steps.[22] The configuration of **10** was again secured by X-ray crystallography (Figure 3, left). The structure nicely shows the bicyclic ring

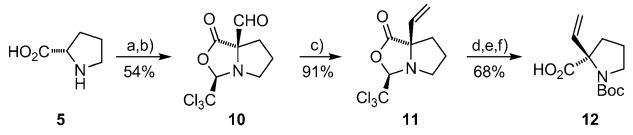

Scheme 3. Synthesis of **12**. a) Cl_3CCHO (2 equiv), MeCN, RT, 15 h; b) LiCl, LDA, HCO_2Me, THF, −78 °C, 30 min; c) $MePPh_3Br$, KO*t*Bu, toluene, 80 °C, 2 h, then **10**, RT, 1 h; d) AcCl (10 equiv), MeOH, RT, 7 days; e) Boc_2O, DIPEA, CH_2Cl_2, RT, 2.5 days; f) LiOH, THF/MeOH/H_2O, 50 °C, 5 h.

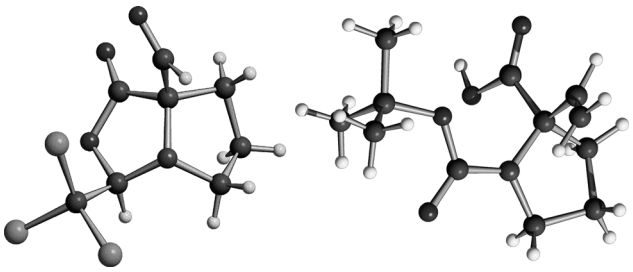

Figure 3. Structure of the 2-formylproline derivative **10** (left) and of *N*-Boc-2-vinylproline (**12**; right) in the crystalline state.

system in a *cisoid* configuration with the CCl_3 substituent in the *exo* (pseudoequatorial) position.

The conversion of aldehyde **10** into vinyl derivative **11** through a Wittig reaction was achieved in 91% yield by using thoroughly dried $MePPh_3Br$ (140 °C, high vacuum, 48 h) (lit.:[22] 74%). The final conversion of **11** into the N-Boc-protected 2-vinylproline **12** was initiated by treatment with an excess of AcCl in MeOH. The resulting crude 2-vinylproline methyl ester was redissolved in dichloromethane and treated with Boc_2O in the presence of Hünig's base. After purification, the N-Boc-protected methyl ester intermediate was hydrolyzed with LiOH in a solvent mixture of MeOH/THF/H_2O to afford **12** in good overall yield (33% over 6 steps). The structure of **12** was secured by X-ray analysis (Figure 3, right) and showed that the pyrrolidine ring adopted an envelope conformation with the central methylene unit in an out-of-plane position (to minimize Pitzer strain).

We next attempted to conclude the planned synthesis of the spirocyclic scaffold **1** (Scheme 1) by peptide coupling of the two building blocks **9** and **12** and subsequent RCM (Scheme 4).

However, we recognized that the coupling of sterically hindered acid **12** with the (bulky) secondary amine **9** represented

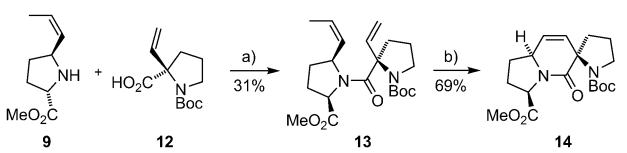

Scheme 4. Unexpected epimerization during the coupling of **9** and **12**. a) 2-(1*H*-7-Azabenzotriazol-1-yl)-1,1,3,3-tetramethyluronium hexafluorophosphate (HATU), *N*,*N*-diisopropylethylamine (DIPEA), NMP, 85 °C, 24 h; b) Grubbs II catalyst (30 mol%), CH_2Cl_2, microwave (300 W), 55 °C, 7 h.

a rather difficult task. By using HATU[25] as a coupling agent in the presence of Hünig's base (DIPEA) in *N*-methyl-2-pyrrolidone (NMP),[26] and heating the mixture for 24 h to 85 °C, we succeeded in obtaining a dipetidic product (**13**) in at least 31% yield. To our surprise, epimerization at the ester-substituted stereocenter occurred during peptide coupling, as unequivocally proven by X-ray crystal-structure analysis at the stage of the metathesis product **14** (Figure 4, left).

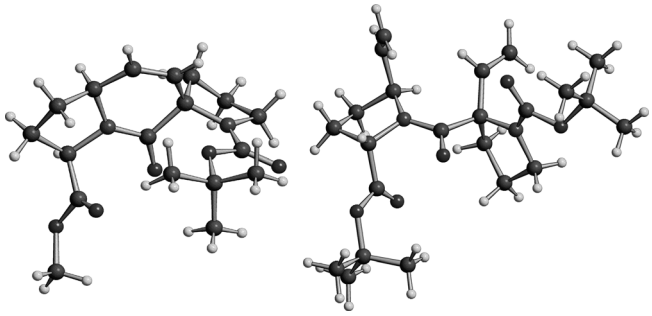

Figure 4. Structures of **14** (left) and **18** (right) in the crystalline state.

The metathesis of **13** was also difficult. Nevertheless, by using 30 mol% of Grubbs II catalyst under microwave conditions[27] (300 W, closed vessel), we could obtain product **14** in 69% yield (in addition to 30% of unreacted **13**).

To optimize the peptide-coupling step, we decided to switch to *tert*-butyl ester **17** (instead of **9**), with the hope that additional steric hindrance would reduce the kinetic acidity of the α-ester position to suppress epimerization. This building block (**17**) was available in gram amounts, starting from the easily accessible methoxylated proline derivative **15**,[12b,18,19a] which was reacted with a vinyl cuprate reagent, according to a procedure reported by Nagaike et al.,[19c] to give **16** as a pure *trans* diastereomer. Cleavage of the N-Boc group with trimethylsilyl trifluoromethanesulfonate (TMSOTf) in CH_2Cl_2 then smoothly afforded the *trans*-2,5-disubstituted pyrrolidine **17** in 67% overall yield (Scheme 5).

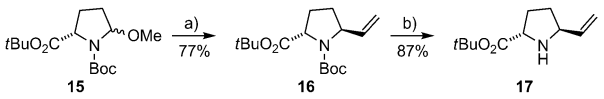

Scheme 5. Synthesis of the *trans*-5-vinylproline **17**: a) CuBr·SMe_2, MgBrCH=CH_2, −40 °C, −78 °C, BF_3·Et_2O, −78 °C, 2 h, RT, 2 h; b) TMSOTf, CH_2Cl_2, 0 °C, 5 min.

Coupling of the building blocks **12** and **17** under the established conditions (HATU, DIPEA) gave rise to a product (**18**) that contained only minor amounts of the undesired isomer *epi*-**18** (**18**/*epi*-**18** = 6:1). Epimerization could even be completely suppressed by reducing the amount of DIPEA to 1.98 equivalents. The optimized protocol delivered stereochemically pure dipeptide **18** in a notable yield of 72%, even on a gram scale (Scheme 6). The configuration of **18** was secured by X-ray crystallography (Figure 4).

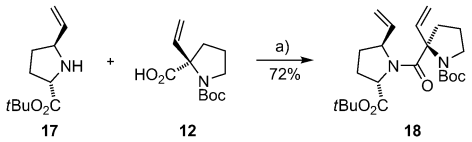

Scheme 6. Coupling of the building blocks **17** (2 equiv) and **12**. a) HATU (1.1 equiv), DIPEA (1.98 equiv), NMP, 85 °C, 24 h.

The importance of minimizing the amount of base in the (difficult) peptide-coupling step is reflected by the fact that coupling product **18** epimerizes under the reaction conditions in the presence of base. Thus, when a solution of pure **18** in NMP was heated in the presence of two equivalents of DIPEA (in the absence of the coupling reagent) to 85 °C for 20 h, virtually complete epimerization to *epi*-**18** was observed (Figure 5). Clearly, the *cis*-2,5-disubstituted pyrrolidine derivative *epi*-**18** is the thermodynamically more stable diastereomer.

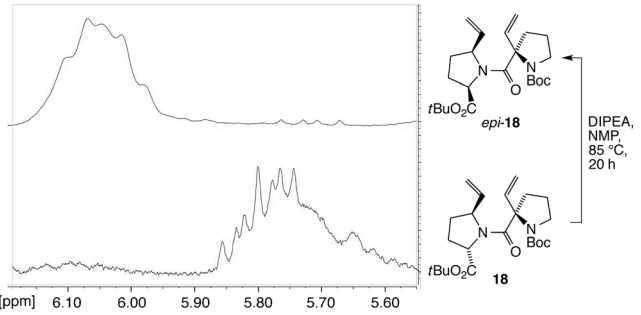

Figure 5. Epimerization of **18** to *epi*-**18**. The signals depicted in the NMR spectrum correspond to the CH group of the vinyl moiety at the ("left") 2,5-disubstituted pyrrolidine ring.

Although epimerization can occur (as shown) at the stage of the coupling products (to give **13** or *epi*-**18**, respectively), we cannot exclude that the amine building block **9** epimerizes under the coupling conditions, followed by a (kinetically preferred)[26] reaction of the less hindered *cis*-2,5-disubstituted pyrrolidine, to directly yield the epimerized product **13** (Scheme 4).

The remaining major task in the synthesis of **1** was metathesis cyclization of **18** to **19** (Scheme 7). This was initially achieved in 68% yield by employing either 30 mol% of Grubbs II catalyst (15 h) or 5 mol% of the nitro-Grela catalyst (72 h). Notably, the yield of **19** could be further improved by performing the reaction in Et_2O with 5 mol% of Grubbs II catalyst in the presence of 7.5 mol% of CuI.[30] Global deprotection and subsequent Fmoc protection under the established conditions[12] finally delivered **1**, that is, the ProM-2-related target structure, in 97% yield.

The configuration of **19** was secured by X-ray crystal-structure analysis (Figure 6). A crystal structure was also obtained from the epimeric compound *epi*-**19** (prepared by metathesis of a 6:1 mixture of **19** and *epi*-**19** and subsequent chromatographic separation of the product diastereomers). The struc-

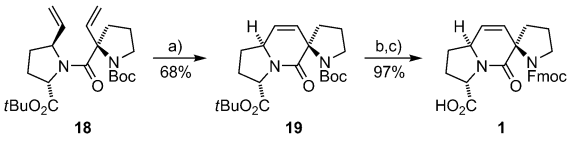

Scheme 7. Synthesis of **1**. a) Grubbs II catalyst (30 mol%), toluene, reflux, 15 h; b) TFA/CH_2Cl_2 1:1, RT, 1 h; c) Fmoc-Cl, $NaHCO_3$, H_2O/THF, RT, 15 h.

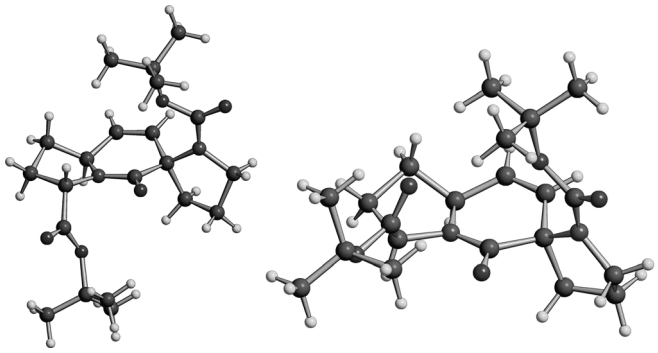

Figure 6. Structure of the tricyclic compounds **19** (left) and *epi*-**19** (right) in the crystalline state. The conformation of **19** almost perfectly matches that of the PPII-helix structure.

ture nicely shows that the diproline unit of **19** is locked in a virtually perfect PPII-type conformation, as predicted. In contrast, compound *epi*-**19** can be regarded as a β-turn mimetic.[22]

Polymorphism of 14

An interesting observation made during this study concerned the occurrence of polymorphs[31] of compound **14** (Scheme 4), which we obtained in crystalline form. As mentioned previously, X-ray crystal-structure analysis of a crystal picked from the sample revealed the formation of unexpected (epimerized) product **14**. To rule out the possibility that we might have accidentally picked a crystal of the minor diastereomer present in the mixture, we investigated a second crystal (with different cell parameters); however, this also corresponded to product **14**. We then even found a third polymorph of **14** in the same sample. All three polymorphs of **14** crystallized in the same space group ($P2_12_12_1$). The cell constants are given in Table 1.

Table 1. Cell constants of the three polymorphs of **14**.

Parameter	Polymorph 1	Polymorph 2	Polymorph 3
a [Å]	7.007	8.944	9.983
b [Å]	15.229	13.539	11.188
c [Å]	17.490	15.249	16.360

Because no solvent molecules were incorporated in any of the three structures, it was of interest to investigate whether the polymorphism originated from conformational or packing effects. A comparison of the three different polymorphs of **14** (Figure 7)[32] clearly revealed that the molecules adopted virtually the same conformation in all three structures. Thus, the polymorphism of compound **14** seems to result just from different packing of the molecules within the crystal.[33]

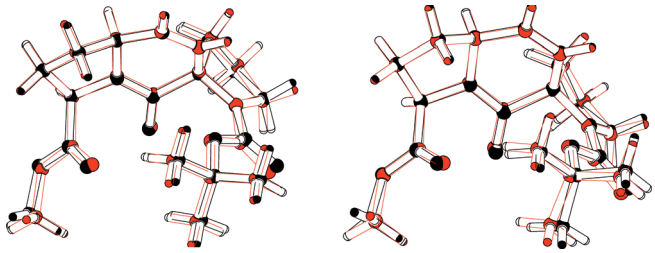

Figure 7. Superimposed structures of **14**. Left: polymorph 1 (black) superimposed with polymorph 3 (red). Right: polymorph 2 (black) superimposed with polymorph 3 (red). This figure was created by using the program PLATON.[32]

Binding studies

As mentioned previously, the main motivation of this work was the search for PPII secondary-structure mimetics that bind to EVH1 domains of the Ena/VASP proteins.[34,35] Herein, we focused on the EVH1 domain of EnaH, which is the human version of the protein Ena, because modeling was performed by using the crystal structure of this domain.

By using standard methods of solid-phase peptide synthesis, the ActA-derived model ligand (Ac-SFE-F**PP**PP-TEDEL-NH_2) and two derivatives, in which the first two proline residues were substituted by either ProM-1 or ProM-2, were prepared and their binding affinity towards EnaH-EVH1 was determined by using tryptophan-based fluorescence titration (FT) and isothermal titration calorimetry (ITC), respectively. As the results shown in Table 2 reveal, exchange of the Pro–Pro unit within the model ligand for either ProM-1 or ProM-2 did not lead to a loss of affinity.

The very similar affinities may reflect the contribution of the flanking epitopes (SFE and TEDEL) to compensate for the less favorable position of the ProM-1 vinylidene bridge in this case (see the Design section). Notably, we could confirm through ^1H–^{15}N HSQC NMR spectroscopy[36] that the ProM-1 and ProM-2

Table 2. Binding data for peptides of type Ac-SFE-F[**XX**]PP-TEDEL-NH_2[a] against EnaH-EVH1 determined either by using tryptophan-based FT or ITC at 25 °C.

	Pro–Pro	ProM-1	ProM-2
FT			
K_D [μM]	13.1 ± 0.6	8.0 ± 1.0	12.0 ± 1.0
ΔG° [kJ mol^{-1}]	−27.9 ± 0.1	−29.1 ± 0.3	−28.1 ± 0.3
ITC			
K_D [μM]	21 ± 1	24 ± 3	21 ± 5
ΔG° [kJ mol^{-1}]	−26.7 ± 0.1	−26.4 ± 0.4	−26.7 ± 0.8
ΔH° [kJ mol^{-1}]	−21.2 ± 0.3	−21.8 ± 0.6	−17.0 ± 2.0
$-T\Delta S^\circ$ [kJ mol^{-1}]	−5.5 ± 0.4	−5.0 ± 1.0	−10.0 ± 2.0

[a] **XX** = Pro–Pro, ProM-1, or ProM-2.

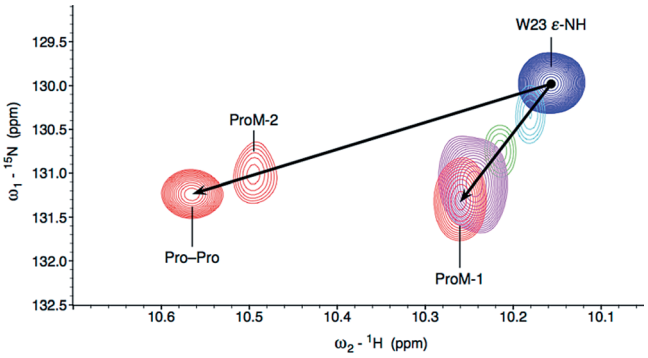

Figure 8. Ligand-concentration-dependent ^{1}H–^{15}N HSQC chemical shifts for W23 ε-NH (of EnaH-EVH1) for the three ligands investigated. A strong slow-exchange regime for the "wild-type" ActA-derived ligand and the ProM-2-containing ligand was observed, whereas for the ProM-1-containing ligand a moderate fast-exchange regime was observed. The blue spot corresponds to the protein in the absence of any ligand, whereas the red spots correspond to protein–ligand concentrations of 98 (model ligand) and 95% (ProM-1 and ProM-2 ligands). The spots in between correspond to protein–ligand concentrations of 25, 50, and 75%, as computed with the dissociation constant determined by tryptophan-based FT (Table 2).

ligands addressed the same binding groove as that of the ActA-derived model peptide (Figure 8).

Moreover, we could detect a difference in the binding modes for the ProM-1- and ProM-2-derived ligands in the ^{1}H–^{15}N HSQC spectra. All ligands connect to the indol moiety of Trp23 of EnaH-EVH1 by forming a hydrogen bond between the ε-NH of the tryptophan side chain and the "central carbonyl oxygen" of the ligand, that is, the central amide group that connects the two pairs of prolines within the **PP-PP** motif of the wild-type ligand (or the central amide bond of the **ProM-PP** moiety in the modified ligands; cf. Figure 2). Although the ProM-2-derived ligand showed the same chemical shift and slow-exchange regime as the model peptide, the ProM-1 ligand shifted differently and in a moderate fast-exchange regime (Figure 9). This indicates a change in the important contact to Trp23 for the different ligands, as suggested by molecular modeling (Figure 2).

Conclusion

We developed a reliable synthesis of the new spirocyclic Pro–Pro dipeptide mimetic ProM-2 in its Fmoc-protected form (**1**), which was designed as a diproline unit locked in a PPII helix conformation. By using vinylproline derivatives as key building blocks, the target structure was assembled through HATU-mediated peptide coupling and subsequent ruthenium-catalyzed RCM. The developed synthesis allowed us to prepare target compound **1** on a gram scale with about 14% overall yield over 10 steps (longest linear sequence), starting from proline. After incorporation of ProM-2 into a model peptide known to bind to the EVH1 domain of Ena/VASP proteins, FT and ITC measurements revealed that the new scaffold was able to replace the highly conserved first two prolines of the model ligand without loss in affinity. Furthermore, ^{1}H–^{15}N HSQC spectra indicated that ProM-2 better mimicked the Pro–Pro unit in this case, relative to the isomeric scaffold ProM-1.

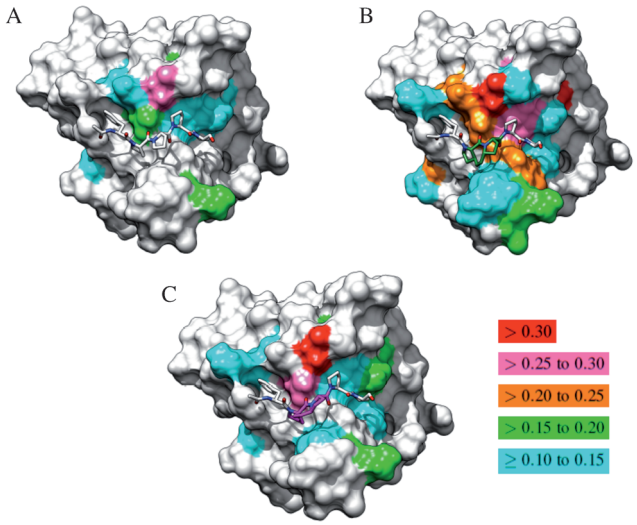

Figure 9. Chemical shifts of all trackable backbone NH protons plotted on: A) the crystal structure of 1evh,[17] B) the model of EnaH-EVH1 with ProM-1, or C) the ProM-2-containing ligand. Only the FPPPP core motif is displayed. The shifts show that the ProM-1- and ProM-2-derived ligands occupy the same binding groove as the model ligand. More shifts are visible for the ProM-1 ligand, which indicates more complex binding behavior than those of the model ligand and ProM-2 ligand.

The scaffold ProM-2 described herein is an important addition to our set of proline-derived polycyclic dipeptide mimetics (ProMs) recently developed in our laboratories.[12] We are optimistic that the modular combination of different ProMs will enable us to identify PPII secondary-structure mimetics that are able to effectively and selectively bind to PRDs, that is, protein domains specialized in recognizing proline-rich motifs in a PPII conformation. Moreover, the difunctional compounds (including the epimeric scaffold *epi*-**18**, to which stereoselective access was discovered by accident) may also find future applications as stereodefined scaffolds for the diversity-oriented synthesis of meaningful compound libraries.

Acknowledgements

This work was supported by the Deutsche Forschungsgemeinschaft (DFG FOR 806). Valuable gifts of chemicals from Rockwood-Lithium GmbH and Evonik are gratefully acknowledged. We also would like to thank Prof. G. Schwarz for access to an Oxford Diffraction Supernova diffractometer and Kai Wirz for the chromatographic purification of **1** on a Grace Reveleris Flash system.

Keywords: amino acids · conformation analysis · helical structures · protein–protein interactions · peptidomimetics

[1] a) B. N. Bullock, A. L. Jochim, P. S. Arora, *J. Am. Chem. Soc.* **2011**, *133*, 14220–14223; for selected reviews, see: b) O. Keskin, A. Gursoy, B. Ma, R. Nussinov, *Chem. Rev.* **2008**, *108*, 1225–1244; c) D. González-Ruiz, H. Gohlke, *Curr. Med. Chem.* **2006**, *13*, 2607–2625; d) Y. Pommier, J. Cherfils, *Trends Pharmacol. Sci.* **2005**, *26*, 138–145; e) A. Reayi, P. Arya, *Curr. Opin. Chem. Biol.* **2005**, *9*, 240–247; f) T. Berg, *Angew. Chem. Int. Ed.* **2003**, *42*, 2462–2481; *Angew. Chem.* **2003**, *115*, 2566–2586.

[2] For selected recent reviews, see: a) M. Jesus Pérez de Vega, M. Martín-Martínez, R. González-Muñiz, *Curr. Top. Med. Chem.* **2007**, *7*, 33 – 62; b) J. Vagner, H. Qu, V. J. Hruby, *Curr. Opin. Chem. Biol.* **2008**, *12*, 292 – 296; c) A. Grauer, B. König, *Eur. J. Org. Chem.* **2009**, 5099 – 5111; d) J. M. Mason, *Future Med. Chem.* **2010**, *2*, 1813 – 1822.

[3] For selected references, see: a) R. E. Moellering, M. Cornejo, T. N. Davis, C. Del Bianco, J. C. Aster, S. C. Blacklow, A. L. Kung, D. G. Gilliland, G. L. Verdine, J. E. Bradner, *Nature* **2009**, *462*, 182 – 190; b) E. Ko, J. Liu, L. M. Perez, G. Lu, A. Schaefer, K. Burgess, *J. Am. Chem. Soc.* **2011**, *133*, 462 – 477; c) J. H. Lee, Q. Zhang, S. Jo, S. C. Chai, M. Oh, W. Im, H. Lu, H.-S. Lim, *J. Am. Chem. Soc.* **2011**, *133*, 676 – 679.

[4] a) L. Ball, R. Kühne, J. Schneider-Mergener, H. Oschkinat, *Angew. Chem. Int. Ed.* **2005**, *44*, 2852 – 2869; *Angew. Chem.* **2005**, *117*, 2912 – 2930; b) *Protein – Protein Interactions as New Drug Targets* (Eds.: E. Klussmann, J. Scott), Handbook of Experimental Pharmacology, Vol. 186, Springer, Heidelberg, **2008**.

[5] a) L. Ball, R. Kühne, B. Hoffmann, A. Häfner, P. Schmieder, R. Volkmer-Engert, M. Hof, M. Wahl, J. Schneider-Mergener, U. Walter, H. Oschkinat, T. Jarchau, *EMBO J.* **2000**, *19*, 4903 – 4914; b) R. Aasland, C. Abrams, C. Ampe, L. Ball, M. Bedford, G. Cesareni, M. Gimona, J. Hurley, T. Jarchau, V. Lehto, M. Lemmon, R. Linding, B. Mayer, M. Nagai, M. Sudol, U. Walter, S. Winder, *FEBS Lett.* **2002**, *513*, 141 – 144; c) L. Ball, T. Jarchau, H. Oschkinat, U. Walter, *FEBS Lett.* **2002**, *513*, 45 – 52.

[6] I. Geisler, J. Chmielewski, *Bioorg. Med. Chem. Lett.* **2007**, *17*, 2765 – 2768.

[7] a) M. Dustin, M. Olszowy, A. Holdorf, J. Bromley, N. Desai, P. Widder, F. Rosenberger, P. van der Merwe, P. Allen, A. Shaw, *Cell* **1998**, *94*, 667 – 677; b) V. Laurent, T. Loisel, B. Harbeck, A. Wehman, L. Gröbe, B. Jockusch, J. Wehland, F. Gertler, M. Carlier, *J. Cell. Biol.* **1999**, *144*, 1245 – 1258.

[8] A. Goldstrohm, T. Albrecht, C. Suñé, M. Bedford, M. Garcia-Blanco, *Mol. Cell. Biol.* **2001**, *21*, 7617 – 7628.

[9] a) B. Laggerbauer, S. Liu, E. Makarov, H.-P. Vornlocher, O. Makarova, D. Ingelfinger, T. Achsel, R. Lührmann, *RNA* **2005**, *11*, 598 – 608; b) M. Kofler, M. Schuemann, C. Merz, D. Kosslick, A. Schlundt, A. Tannert, M. Schaefer, R. Luhrmann, E. Krause, C. Freund, *Mol. Cell. Proteomics* **2009**, *8*, 2461 – 2473.

[10] a) C. M. Deber, F. A. Bovey, J. P. Carver, E. R. Blout, *J. Am. Chem. Soc.* **1970**, *92*, 6191 – 6198; b) N. Helbecque, M. H. Loucheux-Lefebvre, *Int. J. Peptide Protein Res.* **2009**, *19*, 94 – 101; c) H. Okabayashi, T. Isemura, S. Sakakibara, *Biopolymers* **1968**, *6*, 323 – 330; d) R. K. Dukor, T. A. Kiederling, *Biopolymers* **1991**, *31*, 1747 – 1761; e) R. K. Dukor, T. A. Kiederling, V. Gut, *Int. J. Peptide Protein Res.* **2009**, *38*, 198 – 203; f) P. M. Cowan, S. McGavin, *Nature* **1955**, *176*, 501 – 503.

[11] R. Kühne, H. Oschkinat, C. Brockmann, H.-G. Schmalz, **2008**, GER, WO 2008/040332A1.

[12] a) J. Zaminer, C. Brockmann, P. Huy, P. Opitz, C. Reuter, M. Beyermann, C. Freund, M. Müller, H. Oschkinat, R. Kühne, H.-G. Schmalz, *Angew. Chem. Int. Ed.* **2010**, *49*, 7111 – 7115; *Angew. Chem.* **2010**, *122*, 7265 – 7269; b) C. Reuter, P. Huy, J.-M. Neudörfl, R. Kühne, H.-G. Schmalz, *Chem. Eur. J.* **2011**, *17*, 12037 – 12044; c) C. Reuter, M. Kleczka, S. de Mazancourt, J.-M. Neudörfl, R. Kühne, H.-. Schmalz, *Eur. J. Org. Chem.* **2014**, 2664 – 2667; d) A. Soicke, C. Reuter, M. Winter, J.-M. Neudörfl, N. Schlörer, R. Kühne, H.-G. Schmalz, *Eur. J. Org. Chem.* **2014**, 6467 – 6480.

[13] a) M. Krause, E. W. Dent, J. E. Bear, J. J. Loureiro, F. B. Gertler, *Annu. Rev. Cell Dev. Biol.* **2003**, *19*, 541 – 564; b) A. S. Sechi, J. Wehland, *Front. Biosci.* **2004**, *9*, 1294 – 1310; c) F. Drees, F. B. Gertler, *Curr. Opin. Neurobiol.* **2008**, *18*, 53 – 59.

[14] a) M. Hamon, H. Bierne, P. Cossart, *Nat. Rev. Microbiol.* **2006**, *4*, 423 – 434; b) J. A. Vázquez-Boland, M. Kuhn, P. Berche, T. Chakraborty, G. Domínguez-Bernal, W. Goebel, B. González-Zorn, J. Wehland, J. Kreft, *Clin. Microbiol. Rev.* **2001**, *14*, 584 – 640; c) M. B. Goldberg, *Microbiol. Mol. Biol. Rev.* **2001**, *65*, 595 – 626.

[15] R. Opitz, Inhibition von Protein – Protein-Wechselwirkungen, Dissertation, FU-Berlin, **2013**.

[16] Sybyl-X Molecular Modelling suite, Certara, L. P.

[17] K. E. Prehoda, D. J. Lee, W. A. Lim, *Cell* **1999**, *97*, 471 – 480.

[18] a) T. Shono, H. Hamaguchi, Y. Matsumura, *J. Am. Chem. Soc.* **1975**, *97*, 4264 – 4268; b) T. Shono, *Tetrahedron* **1984**, *40*, 811 – 850; c) M. Skrinjar, L.-G. Wistrand, *Tetrahedron* **1991**, *47*, 573 – 582.

[19] For related transformations with 1-propenyllithium-based cuprates, see: a) K. F. McClure, P. Renold, D. S. Kemp, *J. Org. Chem.* **1995**, *60*, 454 – 457; b) E. Grovenstein Jr., K. W. Black, S. C. Goel, R. L. Hughes, J. H. Northrop, D. L. Streeter, D. VanDerveer, *J. Org. Chem.* **1989**, *54*, 1671 – 1679; c) F. Nagaike, Y. Onuma, C. Kanazawa, H. Hojo, A. Ueki, Y. Nakahara, Y. Nakahara, *Org. Lett.* **2006**, *8*, 4465 – 4468.

[20] D. Rodríguez, M. Mulero, J. A. Prieto, *J. Org. Chem.* **2006**, *71*, 5826 – 5829.

[21] a) M. E. Jung, M. A. Lyster, *J. Chem. Soc. Chem. Commun.* **1978**, 315 – 316; b) R. S. Lott, V. S. Chauhan, C. H. Stammer, *J. Chem. Soc. Chem. Commun.* **1979**, 495 – 496; c) F. Manfré, J. M. Kern, J. F. Biellmann, *J. Org. Chem.* **1992**, *57*, 2060 – 2065.

[22] a) H. Bittermann, P. Gmeiner, *J. Org. Chem.* **2006**, *71*, 97 – 102; b) H. Bittermann, F. Böckler, J. Einsiedel, P. Gmeiner, *Chem. Eur. J.* **2006**, *12*, 6315 – 6322.

[23] H. Wang, J. P. Germanas, *Synlett* **1999**, *1*, 33 – 36.

[24] a) D. Seebach, M. Boes, R. Naef, W. B. Schweizer, *J. Am. Chem. Soc.* **1983**, *105*, 5390 – 5398; for a review, see: b) D. Seebach, A. R. Sting, M. Hoffmann, *Angew. Chem. Int. Ed. Engl.* **1996**, *35*, 2708 – 2748; *Angew. Chem.* **1996**, *108*, 2881 – 2921.

[25] a) L. A. Carpino, *J. Am. Chem. Soc.* **1993**, *115*, 4397 – 4398; b) L. A. Carpino, A. El-Faham, F. Albericio, *Tetrahedron Lett.* **1994**, *35*, 2279 – 2282; for reviews on peptide coupling, see: c) A. El-Faham, F. Albericio, *Chem. Rev.* **2011**, *111*, 6557 – 6602; d) C. A. G. N. Montalbetti, V. Falque, *Tetrahedron* **2005**, *61*, 10827 – 10852.

[26] G. Lesma, A. Colombo, A. Sacchetti, A. Silvani, *Tetrahedron Lett.* **2008**, *49*, 7423 – 7425.

[27] For reviews on microwave-assisted synthesis, see: a) C. O. Kappe, *Angew. Chem. Int. Ed.* **2004**, *43*, 6250 – 6284; *Angew. Chem.* **2004**, *116*, 6408 – 6443; b) A. de La Hoz, A. Diaz-Ortiz, A. Moreno, *Chem. Soc. Rev.* **2005**, *34*, 164 – 178; c) Y. Coquerel, J. Rodriguez, *Eur. J. Org. Chem.* **2008**, 1125 – 1132.

[28] a) P. Huy, H.-G. Schmalz, *Synthesis* **2011**, 954 – 960; b) P. G. M. Wuts, T. W. Greene, *Greene's Protective Groups in Organic Synthesis*, 4th ed., Wiley-Interscience **2007**.

[29] G. Sunilkumar, D. Nagamani, N. P. Argade, K. N. Ganesh, *Synthesis* **2003**, *15*, 2304 – 2306.

[30] K. Voigtritter, S. Ghorai, B. H. Lipshutz, *J. Org. Chem.* **2011**, *76*, 4697 – 4702.

[31] a) J. Bernstein, *Polymorphism in Molecular Crystals*, Clarendon, Oxford, **2002**; b) R. Purohit, P. Venugopalan, *Resonance* **2009**, *14*, 882 – 893.

[32] A. L. Spek, *Acta Crystallogr. Sect. D* **2009**, *65*, 148 – 155.

[33] CCDC-1042396 (*Z*-**9**), 1042403 (**10**), 1042402 (**12**), 1042397 (**14**, polymorph 1), 1042400 (**14**, polymorph 2), 1042401 (**14**, polymorph 3), 1042399 (**18**), 1042395 (**19**), and 1042398 (*epi*-**19**) contain the supplementary crystallographic data for this paper. These data can be obtained free of charge from the Cambridge Crystallographic Data Center via www.ccdc.cam.ac.uk/data_request/cif.

[34] a) E. T. Roussos, M. Balsamo, S. K. Alford, J. B. Wyckoff, B. Gligorijevic, Y. Wang, M. Pozzuto, R. Stobezki, S. Goswami, J. E. Segall, D. A. Lauffenburger, A. R. Bresnick, F. B. Gertler, J. S. Condeelis, *J. Cell Sci.* **2011**, *124*, 2120 – 2131; b) F. Di Modugno, M. Mottolese, L. DeMonte, P. Trono, M. Balsamo, A. Conidi, E. Melucci, I. Terrenato, F. Belleudi, M. R. Torrisi, M. Alessio, A. Santoni, P. Nisticò, *PLoS ONE* **2010**, *5*, e15852; c) A. Toyoda, H. Kawana, K. Azuhata, J. Yu, A. Omata, H. Kishi, M. Higashi, K. Harigaya, *Int. J. Oncol.* **2009**, *34*, 53 – 60; d) S. Goswami, U. Philippar, D. Sun, A. Patsialou, J. Avraham, W. Wang, F. Di Modugno, P. Nisticò, F. B. Gertler, J. S. Condeelis, *Clin. Exp. Metastasis* **2009**, *26*, 153 – 159; e) U. Philippar, E. T. Roussos, M. Oser, H. Yamaguchi, H.-D. Kim, S. Giampieri, Y. Wang, S. Goswami, J. B. Wyckoff, D. A. Lauffenburger, E. Sahai, J. S. Condeelis, F. B. Gertler, *Development* **2008**, *15*, 813 – 828.

[35] J. H. Holtzman, K. Woronowicz, D. Golemi-Kotra, A. Schepartz, *Biochemistry* **2007**, *46*, 13541 – 13553.

[36] P. Schanda, E. Kupce, B. Brutscher, *J. Biomol. NMR* **2005**, *33*, 199 – 211.

Received: December 15, 2014
Revised: March 11, 2015
Published online on April 23, 2015

